ISSN: 2347-467X, Vol. 13, No. (2) 2025, Pg. 651-666

Current Research in Nutrition and Food Science

www.foodandnutritionjournal.org

Protective effect of the Leaves of *Bergenia scopulosa* on Oxidative Damage by UHPLC-Q Exactive Focus MS, Network Pharmacology and Molecular Docking

HUI REN, WENJING LU, XIAOMIN CUI, JING HU and ZHIYONG CHEN*

Shaanxi Academy of Traditional Chinese Medicine, Xi'an Shaanxi, China.

Abstract

The rhizomes of *Bergenia scopulosa*, known as dapanlongqi, have been widely used as an Taibai Seven Medicine in the folk medicine of China. However, its leaves, considered a non-medicinal part, have not been extensively studied. This research aims to explore the chemical composition and pharmacological activities of *B. scopulosa* leaves, providing new insights for the comprehensive utilization of the plant. In this study, a total of 59 compounds, including 13 flavonoids, 7 isocoumarins, 35 phenolic acids and 4 others were tentatively characterized in the leaves of *B. scopulosa* by ultra-high performance liquid chromatography coupled with Q exactive focus mass spectrometry (UHPLC-Q Exactive Focus MS). All the known compounds were reported from the leaves of *B. scopulosa* for the first time. The *B. scopulosa* leaves contained abundant and structurally diverse phenolics, and exhibited similar $DPPH^{\cdot}$ and $ABTS^{\cdot+}$ scavenging abilities with trolox. Network pharmacology and molecular docking analyses identified astragalin, reynoutrin, rutin, luteolin, ellagic acid, kaempferol, and catechin as the primary antioxidants in the leaves. This study is the first to comprehensively characterize the chemical composition and antioxidant properties of *B. scopulosa* leaves and reveals their potential in treating atherosclerosis, neurodegeneration, infections, inflammation, and diabetic complications. The research emphasizes the importance of utilizing non-medicinal plant parts while promoting sustainable resource use. The identified antioxidants also hold promise for the development of new drugs and health products, addressing oxidative stress-related diseases.

Article History

Received: 23 January 2025

Accepted: 25 April 2025

Keywords

Antioxidants;
*Bergenia Scopulosa L*eaves;
Flavonoids;
Isocoumarins;
Phenolics;
UHPLC-Q Exactive Focus MS.

CONTACT Zhiyong Chen chenzhiyong0612@sina.com Shaanxi Academy of Traditional Chinese Medicine, Xi'an Shaanxi, China.

Doi: https://dx.doi.org/10.12944/CRNFSJ.13.2.8

Abbreviations

UHPLC-Q Exactive Focus MS	Ultra-high performance liquid chromatography coupled with Q exactive focus mass spectrometry
DPPH	2,6-Dichlorophenolindophenol
ABTS	2,2'-Azinobis(3-ethylbenzothiazoline-6-sulfonic acid)
ROS	Reactive oxygen species
NCE	normalized collision energy
TCM	Traditional Chinese medicine
PPI	protein-protein interaction
BC	Betweenness centrality
CC	Closeness centrality
GO	Gene ontology
KEGG	Kyoto encyclopedia of genes and genomes
RNS	Reactive nitrogen species
FDR	False discovery rate
OD	Optical density
SD	Standard deviation
L-C-T	Leave-compound-target
NOS	Nitric oxide synthase

Introduction

Bergenia scopulosa T.P. Wang is a perennial herbaceous plant of Saxifragaceae family, which is endemic to China, including Shaanxi, Sichuan and Gansu province.[1-3] This plant resembles a small Chinese cabbage and grows in the crevices of rocks, often referred to as "rock cabbage". In China, the wild resources of *B. scopulosa* are mainly distributed in the Qinling Mountains,[4] the geographical boundary between the north and south of China, so there is a beautiful Chinese name called "Qinling rock cabbage". In the folk medicine of China, the rhizomes of *B. scopulosa*, also known as dapanlongqi, is one of the famous Taibai Seven Medicines. It is commonly used to treat acute and chronic enterogastritis, cough, hematemesis, hematochezia, edema, metrorrhagia and metrostaxis, leukorrhea, etc.[1,5] The rhizomes of *B. scopulosa* and meat cooked together in soup not only taste delicious, but also treat asthma and dry cough.

Previous studies have demonstrated the presence of structurally diverse isocoumarins and flavonoids in the rhizomes of *B. scopulosa*, alongside phenolics, steroids, glycosides, and amino acids.[6-11] However, the leaves, traditionally considered non-medicinal parts of this plant, remain largely unexplored. Notably, fresh *B. scopulosa* leaves are consumed as vegetables in local diets, where they are believed to possess anti-inflammatory and cooling properties. This dual functionality—edibility and medicinal potential—highlights the underutilized value of leaf tissues. Based on the literature review, it has been found that the research on the leaves is currently very limited. For instance, there is a lack of phytochemical data, limited understanding of its bioactive compounds, and absence of studies on its potential therapeutic applications. In light of this, the study will lay the foundation for the sustainable application of this traditional herbal medicine, the development of potential nutraceuticals, and the expansion of its clinical applications.

Different plant organs often exhibit overlapping chemical profiles and pharmacological activities due to shared biosynthetic pathways. Polyphenols, a class of compounds characterized by one or more aromatic rings with two or more hydroxyl groups, mainly exist in plants, particularly in fruits and vegetables, are recognized for their antioxidant properties. Our previous research has shown that polyphenols are vital components of the rhizomes of *B. scopulosa*, including isocoumarins, flavonoids and phenolic acids.[3,9] Oxidative stress, characterized by an imbalance between the production of reactive oxygen species (ROS) and the plant's antioxidant defense mechanisms, can result in cellular damage and impaired physiological functions. To counteract

this stress, plants have developed sophisticated defense systems, primarily relying on bioactive compounds such as polyphenols, flavonoids, and phenolic acids. Given that oxidative stress is a significant contributor to aging and various diseases, polyphenols play a crucial role as natural antioxidants in mitigating cellular damage. As a powerful technique for plant metabolite profiling, ultra-high performance liquid chromatography coupled with Q exactive focus mass spectrometry (UHPLC-Q Exactive Focus MS) has advantages of high resolution, rapid analysis, and broad detection ranges, which enables rapid identification of antioxidant compounds (e.g., flavonoids, phenolic acids) from plant extracts.[12,13] It is particularly well-suited for identifying both major and trace compounds in the leaves of *B. scopulosa* which may contribute to expanding knowledge in the field of natural product pharmacology. Network pharmacology, based on systems biology principles, predicts therapeutic targets by constructing compound-disease networks and identifying key regulatory nodes (e.g., SIRT1, Nrf2) involved in aging and inflammation. Molecular docking technology subsequently verifies the binding affinity and conformation of bioactive compounds with their target proteins, guiding structure-based drug optimization. Building on these advantages, we conducted this study with three specific objectives: (1) To characterize the phytochemical composition in the leaves of *B. scopulosa* using UHPLC-Q Exactive Focus MS; (2) to screen for bioactive compounds and identify key targets associated with oxidative stress attenuation via network pharmacology; (3) to evaluate the binding affinities of these bioactive compounds to their key targets through molecular docking.

Materials and Methods

Reagents and Materials

The dry leaf material of *B. scopulosa* (No. 20210808) was collected from Taibai Mountain, Baoji City, Shaanxi Province, P.R. China, in Aug 8th, 2021. The plant leaves were authenticated as genuine by Dr. Zhiyong Chen, from Shaanxi Academy of Traditional Chinese Medicine (Xi'an, China). The Shanghai Qiming Bioengineering Institute (Shanghai, China) supplied arbutin, chlorogenic acid, catechin, protocatechuic acid, rutin. Sichuan Weikeqi Biological Technology Co., Ltd. (Chengdu, China) provided gallic acid (wkq20010905). Chengdu Pufei De Biotech Co., Ltd. (Chengdu, China) provided bergenin (20123004), 4-O-galloylbergenin (221104), 11-O-galloylbergenin (22030306), astragalin (21101302), kaempferol-3-O-rutinoside (22041506), cymaroside (18092904), 1,3,6-tri-O-galloylglucose (20092401), isoquercitrin (20112403), kaempferol (20082105) and luteolin (20121604). Epicatechin gallate (HR1130W5) was acquired from Baoji Herbest bio-tech Co., Ltd. (Baoji, China). Epicatechin (MUST-20102910) was purchased from Chengdu Must bio-technology Co., Ltd. (Chengdu, China). Reynoutrin (PS011302) was supplied by the Chengdu Push bio-technology Co., Ltd. (Chengdu, China). Ellagic acid (C11648502), 1,1-Diphenyl2-picrylhydrazyl (DPPH, C14357523), 2,2'-azinobis-(3-ethylbenzthiazoline-6-sulphonate) (ABTS, C14565258), Folin-Ciocalteu reagent (C13547993), casein (C12913946), potassium persulfate (C14951199) were acquired from Shanghai Macklin biochemical Co., Ltd. (Shanghai, China). Methyl gallate (AN1127SA14) was acquired from Shanghai Yuanye Bio-Technology Co., Ltd. (Shanghai, China). 6-Hydroxy-2,5,7,8-tetramethylchroman-2-carboxylic acid (trolox, 1027J021) was purchased from Beijing Solarbio Science & Technology Co., Ltd. (Beijing, China). Methanol HPLC grade and formic acid LC-MS grade were all purchased from Fisher Scientific (Fair Lawn, NJ, USA). Ultrapure water was supplied by Watson's Food and Beverage Co., Ltd. (Guangzhou, China). Identification of the chemical constituents of the leaves of *B. scopulosa* was performed on a Thermo Fisher Scientific UPLC system (UltiMate 3000) coupled to a Q Exactive Focus MS (Thermo Finnigan, San Jose, CA, USA).

UHPLC-Q Exactive Focus MS analysis

The sample preparation protocol was adapted from our previously reported methods as follows:[3,9] A 0.1 g aliquot (60 mesh) of accurately weighed *B. scopulosa* leaves was subjected to ultrasonication in 20 mL of 70 % methanol at 25 °C for 30 minutes. The weight loss during extraction was compensated by adding an equivalent volume of 70% methanol to maintain consistent extract concentration. The supernatant was filtered through 0.22 μm filter membranes to remove particulates prior to UHPLC-Q Exactive Focus MS analysis.

Separation was achieved using a Thermo Accucore aQ RP18 (2.1 mm × 150 mm, 2.6 μm) column maintained at 30 °C. The binary mobile phase

consisted of methanol (A) and 0.1% formic acid in H_2O (B), delivered at a flow rate of 0.3 mL·min^{-1} under a gradient elution program: 0–35 min, 2%–45% (A); 35–50 min, 45%–95% (A); and 50–55 min, 95% (A). The injection volume was set to 2 µL. The MS was configured with a heated electrospray ionization source operating in negative ion mode. The instrument parameters were as follows: spray voltage at 3.0 kV; capillary temperature at 320 °C; sheath gas flow rate at 40 arb; auxiliary gas flow rate at 10 arb; desolvation temperature at 350 °C; normalized collision energy (NCE) at 20, 40 and 60 eV; and S-lens RF level at 50; resolution of 70 000 for MS and 17 500 for MS^2. Data-dependent MS (full MS/dd-MS^2) scanning was employed to acquire fragmentation spectra of target ions within the mass range of m/z 80–1200. Mass data were processed using Xcalibur software (version 4.1, Thermo Fisher Scientific, San Jose, CA, USA). Compound data were compared with the chemical database of *Bergenia* genus, ChemicalBook (https://www.chemicalbook.com), and ChemSpider (http://www.chemspider.com).

Measurement of Phenolics

The leave powder (60 mesh) of *B. scopulosa* were refluxed with 70% ethanol for 1 h. After filtration, the residue was subjected to two additional extractions with 70% ethanol for 1 h each. The filtered supernatants were mixed and evaporated to dryness under reduced pressure at 50 °C.

The resulting extracts were dissolved and diluted to appropriative concentrations for the determination of total phenols and favonoids using the Folin-Ciocalteu method and aluminum chloride colorimetric assay.[14] Condensed tannins were assessed based on phosphomolybdenum tungstic acid-casein reaction described by Xue *et al*.[14] with slight modifications. Briefly, 25 mL appropriately diluted leaf extract was mixed with 600 mg casein and incubated at room temperature for 3 h with continuous vortexing. Following incubation, the mixture was centrifuged at 3000 rpm for 5 min to collect the supernatant, referring to as the sample after CASEIN-Precipitating reaction. The subsequent steps were identical to those used for total phenols determination. Total tannins were calculated as the difference in total phenols between the samples before and after CASEIN-Precipitating Reaction. Each sample was analyzed in triplicate.

Assessment of Antioxidant Activities

The samples obtained in Measurement of Phenolics Section were systematically diluted to different concentrations for the DPPH$^{\bullet}$ scavenging capacity, following the standardized protocol established by Xue *et al*.[14] $ABTS^{\bullet+}$ scavenging activity of *B. scopulosa* leaves was analyzed using the method reported by Xue *et al*.[1] with slight modiffcations. Specifically, the $ABTS^{\bullet+}$ solution was prepared according to the protocol described by He *et al*.[15] In brief, 88 µL potassium persulfate (140 mM) was added to 5 mL freshly prepared $ABTS^{\bullet+}$ (7 mM), and allowed to stand in the dark at room temperature for 12-16 h. The resulting solution was then diluted to obtain an $ABTS^{\bullet+}$ working solution with an absorbance of 0.70 ± 0.02 at 734 nm. The $ABTS^{\bullet+}$ working solution (190 µL) was added to samples (10 µL) at various concentrations. Each treatment was performed in triplicate. After mixing for 10 seconds, the samples were incubated in the dark at 30 °C for 5 minutes. The absorbance was then measured at 734 nm using a microplate reader. The inhibitory rates of $ABTS^{\bullet+}$ scavenging activity were calculated using the following formula: ABTS scavenging rate (%) = $[1 - (OD_{test} - OD_{test\ blank})/(OD_{negative\ control} - OD_{blank]} \times 100$. IC_{50} values were determined and are presented as the means ± SD in micromolar concentrations. The data significance analysis was conducted using a t-test statistical method.

Target Collection

The targets of the compounds derived from the leaves of *B. scopulosa* were identified using TCM systems pharmacology database and analysis platform (TCMSP, https://tcmspw.com/tcmspsearch.php)[16] and the Swiss Target Prediction (http://www.swisstargetprediction.ch/).[17,18] Subsequently, the Universal Protein Resource (UniProt, http://www.uniprot.org/) was employed to standardize the target information of these compounds, with a focus on "Homo sapiens". Additionally, the GeneCards database (https://www.genecards.org)[19] was utilized to gather target information related to oxidative stress, with a filter applied for correlation scores greater than.[10] The potential targets of *B. scopulosa* leaves in mitigating oxidative damage were elucidated by identifying the overlapping targets between the compounds and oxidative stress-related targets.

Network Construction

The protein-protein interaction (PPI) networks of overlap targets were plotted using the STRING (https://string-db.org/),[20] with species set to "Homo Sapiens" and the protein interaction confidence score threshold set to 0.9. Cytoscape 3.9.1 software was adopted to visualize and analyze the network, and the network topology analysis was then performed to screen the key targets of the leaves of *B. scopulosa* on oxidative damage, taking degree, betweenness centrality (BC), and closeness centrality (CC) as screening parameters on oxidative damage. Targets exhibited higher topological values than average were selected as the key targets on oxidative damage. Furthermore, the leaves of *B. scopulosa*, the overlap targets of the compounds and the oxidative stress was imported to Cytoscape 3.9.1 software for generating the leave-compound-target (L-C-T) network construction. The degree, BC and CC were then analyzed to obtain the key bioactive compounds of the leaves of *B. scopulosa* on oxidative damage. Compounds exhibited higher topological values than average were selected as the key bioactive compounds of the leaves of *B. scopulosa* on oxidative damage.

GO and KEGG Pathway Enrichment

"Homo sapiens" was limited to analyse the overlap targets of the compounds and oxidative stress by the Metascape database (https://metascape.org), and "Custom Analysis" was then performed to enrich biological processes, cellular components, molecular functions, and KEGG pathway.

Molecular Docking

Molecular docking was performed among bioactive compounds and key targets using our previously reported methods[21,22] with slight modiffcations. The three-dimensional (3D) structures of key bioactive compounds extracted from the leaves of *B. scopulosa* were obtained in .sdf format from the PubChem database (https://pubchem.ncbi.nlm.nih.gov/), and subsequently converted to .pdb format using OpenBabel 2.4.1.[21] The crystal structures of target proteins were retrieved from the PDB database (https://www.rcsb.org/), where ligands and water molecules were completely removed using Discovery Studio 4.5 to ensure accurate receptor preparation.[21] Set for "Homo sapiens", the protein name is identical to the corresponding gene name, with no mutations and maximal integrity retained. Furthermore, the structure of key bioactive compounds of the leaves of *B. scopulosa* and target proteins were submitted to AutoDockTools 1.5.7 software for hydrogenation and charge assignment, followed by semi flexible docking analysis using AutoDock Vina module with default parameters, yielding up to 10 binding poses.[21,22] The resulting protein-ligand complexes were subsequently analyzed using the protein-ligand interaction profiler (PLIP, https://plip-tool.biotec.tu-dresden.de/plip-web/plip/index) to identify binding site and acting force analysis between ligands and receptors.[23] Finally, PyMOL was utilized for 3D visualization of the binding interfaces, enabling detailed analysis of spatial complementarity and residue-specific interactions.

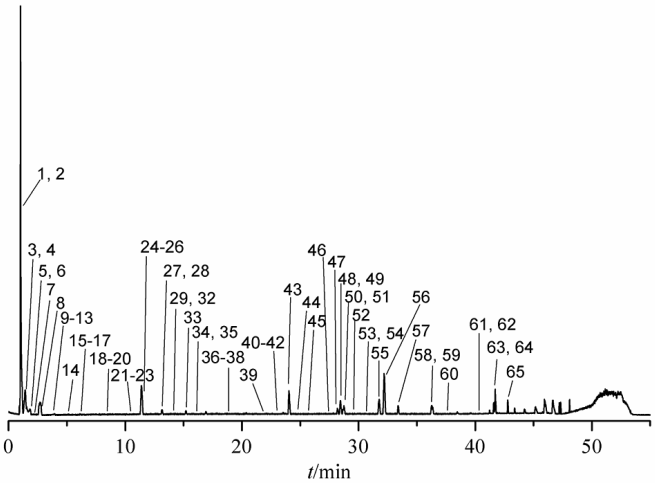

Fig. 1: Base peak chromatogram of the leaves of *Bergenia scopulosa* in negative ion mode

Results

Chemical Profiling of the Leaves of *B. Scopulosa*

The 70% methanol extract of the leaves of *B. scopulosa* was analyzed using the UHPLC-Q Exactive Focus MS method, with the analysis completed within 55 minutes. The base peak intensity chromatogram of the *B. scopulosa* leaf extract in negative ion mode is presented in Figure 1. By comparing the detected compounds with the chemical database of *Bergenia* genus, ChemicalBook, and ChemSpider, a total of 59 compounds were tentatively identified. These include 13 flavonoids, 7 isocoumarins, 35 phenolic acids and 4 other types. Detailed information on these compounds is provided in Table S1.

Flavonoids

A total of 13 compounds were identified as flavonoids, including flavones, flavonols and flavan-3-ols. Compounds 45 and 51 showed an [M-H]- ion at m/z 609.1475 ($C_{27}H_{30}O_{16}$). These were assigned as quercetin-O-rutinoside, the loss of the sugar moiety from the parent ion resulted in a fragment ion at m/z 300.0280, indicating the presence of one rutinose connected with flavonoid skeleton. Compared with the reference standard, compounds 51 was unambiguously identified as rutin, while 45 was an isomer of 51. Similarly, compounds 49 and 56 were characterized as kaempferol-O-rutinoside. In the MS/MS spectrum of compounds 49 and 56, the characteristic fragment ion at m/z 285.0405 indicated the presence of one rutinose unit. Compounds 46 and 55 were also identified as isomers. The directly loss of a glucose molecule from the quasi-molecular ion resulted in a product ion at m/z 285.0405. Compounds 46 and 55 were characterized as cymaroside and astragalin, respectively, by comparing with reference standards. Compound 48 exhibited an [M-H]- ion at m/z 463.0898 ($C_{21}H_{20}O_{12}$). It was assigned as isoquercitrin by comparing with a reference standard, loss of one glucose molecule from the quasi-molecular ion resulted in the fragment ion at m/z 300.0280. Compound 52, with a chemical formula suggesting the presence of one pentose unit attached to quercetin, was identified as reynoutrin by comparison with a reference standard. This identification was supported by the characteristic ion at m/z 301.0342. In addition, compounds 60 and 61 were identified as luteolin and kaempferol by comparing with reference compounds, respectively. Compounds 24 and 35 shared the same formula of $C_{15}H_{14}O_6$. In their MS/MS spectrums, characteristic ions at m/z 151.0403 and 137.0247 were resulted from RDA fragmentation. Moreover, the chemical structure of the ion at m/z 289.0721 was confirmed by the loss of CO_2 molecule and the ion was produced at m/z 245.0820. Compounds 24 and 35 were identified as catechin and epicatechin, respectively, by comparing with reference standards. Compound 39 showed an [M-H]- ion at m/z 441.0828 ($C_{22}H_{18}O_{10}$). The characteristic ions at m/z 289.0720 and 169.0145 were produced via the breaking of the ester bond in the secondary mass spectrum, which implied one galloyl group connected with catechin or epicatechin. Compound 39 was characterized as epicatechin gallate by comparing with a reference standard.

Isocoumarins

A total of 7 isocoumarins were identified from the leaves of *B. scopulosa* sample, including norbergenin, bergenin, 4-O-galloylbergenin, 11-O-galloylbergenin, di-O-galloyl bergenin, p-hydroxybenzoyl bergenin, tri-O-galloyl bergenin. Compound 25 was characterized as bergenin by comparing with a reference standard. Compounds 36 and 43 showed the same formula of $C_{21}H_{20}O_{13}$. The quasi-molecular ion at m/z 479.0837 directly lost the isocoumarin skeleton and resulted in the ion at m/z 169.0145 in the secondary mass spectrum, which implied one galloyl group connected with bergenin. Compounds 36 and 43 were identified as 4-O-galloylbergenin and 11-O-galloylbergenin by comparing with reference standards, respectively. Similarly, the molecular formula of compounds 47 and 54 suggest that two galloyl groups or three galloyl groups are attached to bergenin. Therefore, compounds 47 and 54 were tentatively identified as di-O-galloyl bergenin and tri-O-galloyl bergenin, respectively. Compound 53 was tentatively identified as p-hydroxybenzoyl bergenin.

Phenolic Acids

A total of 35 phenolic acids were identified from the leaves of *B. scopulosa* sample, including O-, C- glycosides and simple organic acid. Phenolic acids were composed of modules such as gallic acid, arbutin, p-hydroxybenzoic acid and ellagic acid in the leaves of *B. scopulosa*. Here we use 42 and 44 as examples to illustrate their structural identifications. They all showed [M-H]- ions at m/z 787.1021 ($C_{34}H_{28}O_{22}$). The quasi-molecular ion

directly lost consecutive galloyl groups and one water molecule resulted in the product ions at m/z 617.0789, 465.0681, and 313.0562. Moreover, the characteristic ions at m/z 169.0143 was resulted from the breaking of the ester bond in the secondary mass spectrum, which also implied galloyl groups in the compounds. Therefore, they were tentatively identified as tetra-O-galloylglucose. Similarly, compounds 31 and 37 showed the same formula of $C_{27}H_{24}O_{18}$. They were tentatively identified as tri-O-galloylglucose according to the characteristic ions at m/z 465.0680, 313.0570, and 169.0143. Furthermore, compound 37 was characterized as 1,3,6-tri-O-galloylglucose by comparing with a reference standard. Compound 40 showed a [M-H]- ion at m/z 391.1043 ($C_{19}H_{20}O_9$). The quasi-molecular ion directly lost one hydroquinone molecule resulted in the product ion at m/z 281.0675. Correspondingly, two characteristic ions at m/z 137.0245 and 109.0296 suggest the presence of hydroxybenzoic acid and hydroquinone parts. Compound 40 was tentatively identified as breynioside A.9 Compounds 11 and 26 were tentatively identified as mallonanoside A and ardimerin,9 respectively, belonging to phenolic C-glycosides. In addition, compounds 5, 8, 14, 20, 28 and 50 were identified as arbutin, gallic acid, protocatechuic acid, methyl gallate, chlorogenic acid and ellagic acid by comparing with reference compounds, respectively.

Others

Compound 1 exhibited a [M-H]- ion at m/z 191.0563 ($C_7H_{12}O_6$), and was tentatively identified as quinic acid. Compound 2 showed a [M-H]- ion at m/z 133.0144 ($C_4H_6O_5$), and was tentatively identified as malic acid. Compound 4 showed a [M-H]- ion at m/z 191.0202 ($C_6H_8O_7$), and was tentatively identified as citric acid. Compound 62 showed a [M-H]- ion at m/z 207.1023 ($C_{12}H_{16}O_3$), and was tentatively identified as anisyl isobutyrate.[9]

Contents and Antioxidant Activities of the Phenolics

Following the identification of phenolic compounds in *B. scopulosa* leaves, the extracts were prepared for quantification of phenolic content and evaluation of antioxidant activity. As shown in Table S2, the extracts exhibited the highest total flavonoid content, followed by total phenols and condensed tannins, respectively. Notably, the extracts displayed lower DPPH IC_{50} values compared to Trolox, indicating potent free-radical scavenging activity. Moreover, their $ABTS^{\cdot+}$ scavenging capacity was comparable to that of Trolox. These results collectively suggest that the total phenolic compounds, particularly flavonoids, play a major role in the observed antioxidant properties of *B. scopulosa* leaf extracts.

Network Construction

Oxidative stress arises from an imbalance between excessive reactive oxygen/nitrogen species (ROS/RNS) production and compromised antioxidant defense systems, leading to cellular damage and dysfunction.[24] To investigate the molecular mechanisms underlying the antioxidant properties of *B. scopulosa* leaves against oxidative damage, we employed network pharmacology and molecular docking approaches. A total of 240 targets were identified from the TCMSP and the Swiss Target Prediction. Additionally, 585 genes associated with oxidative stress were retrieved from the GeneCards database. Through further analysis, 82 potential targets related to oxidative stress for the leaves of *B. scopulosa* were ultimately determined. The detailed information of these 82 genes is presented in Table S3.

The PPI network for the leaves of *B. scopulosa* was constructed using the STRING database (version 11.5), followed by functional enrichment analysis. Following network topology characterization in Cytoscape 3.9.1 (Figure S1), 82 candidate genes associated with oxidative stress responses were imported and filtered to exclude seven lowly connected nodes (MGST1, GSTA1, TYR, AKR1B1, TXNRD1, SERPINE1, PDE5A), resulting in a final dataset comprising 75 core proteins and 586 significant interactions (Table S4). The nodes were arranged from the outside to the inside based on their degree values in descending order. The size and color of the nodes were set to gradually transition from red to yellow according to the degree value, where larger nodes and redder colors indicate higher degree values (Figure S1). This visualization approach leverages Cytoscape's network analysis capabilities to highlight key nodes based on their connectivity, with node size and color mapped to degree values using continuous mapping in the style panel. The average degree was 15.6267, the average BC was 0.0239, and the average CC was 0.3819 for the genes. Targets exhibited higher topological values than the average of certain parameters were

selected as the key targets on oxidative damage: AKT1, SRC, JUN, HSP90AA1, TP53, MAPK1, RELA, MAPK8, ESR1, TNF, IL6, NOS2, and NOS3. These findings suggest that these 13 high centrality proteins may act as pivotal regulators in the plant's antioxidant defense mechanism.

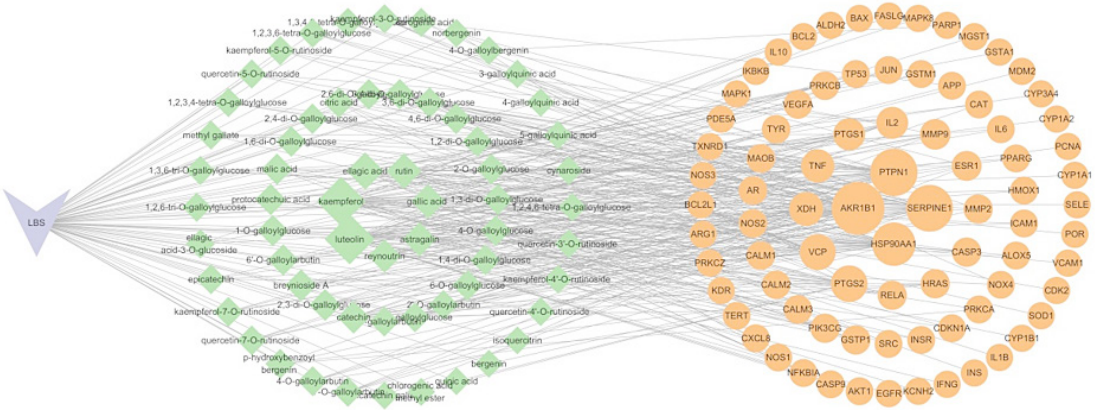

Fig. 2: The leave-compound-target network for the leaves of *Bergenia scopulosa* on oxidative damage

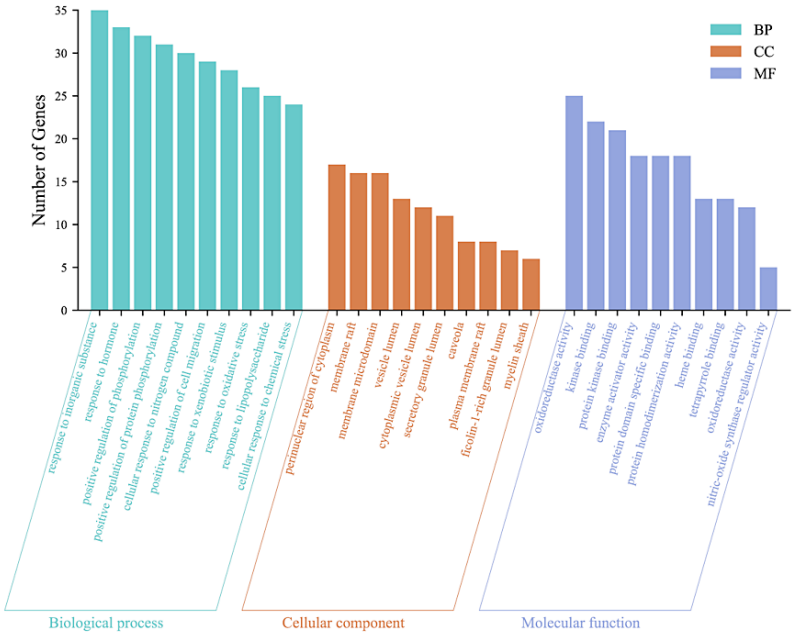

Fig. 3: GO functional enrichment analysis

Furthermore, a L-C-T network comprising 145 nodes and 391 edges was constructed to visualize and analyze the complex interactions between *B. scopulosa* leaves, their bioactive compounds, and oxidative stress-related targets. As illustrated in Figure 2, the network visualizes three components: purple V-shapes representing the plant leaves, green diamonds denoting identified compounds, and orange circles corresponding to potential target proteins. Using Cytoscape 3.9.1's Network Analyzer module, we quantified topological parameters (node degree, BC, CC) for each node (Table S5). The network exhibited an average node degree of 6.3065, average BC of 0.0160, and average CC of 0.4023 among compound nodes. Compounds exhibited higher topological values than the

average of certain parameters were selected as key bioactive compounds of the leaves of *B. scopulosa* on oxidative damage: luteolin, kaempferol, ellagic acid, rutin, gallic acid, astragalin, reynoutrin, catechin, malic acid, and protocatechuic acid. These compounds are predicted to modulate key pathways such as NF-κB signaling and mitochondrial redox homeostasis, highlighting their synergistic potential in mitigating oxidative damage.

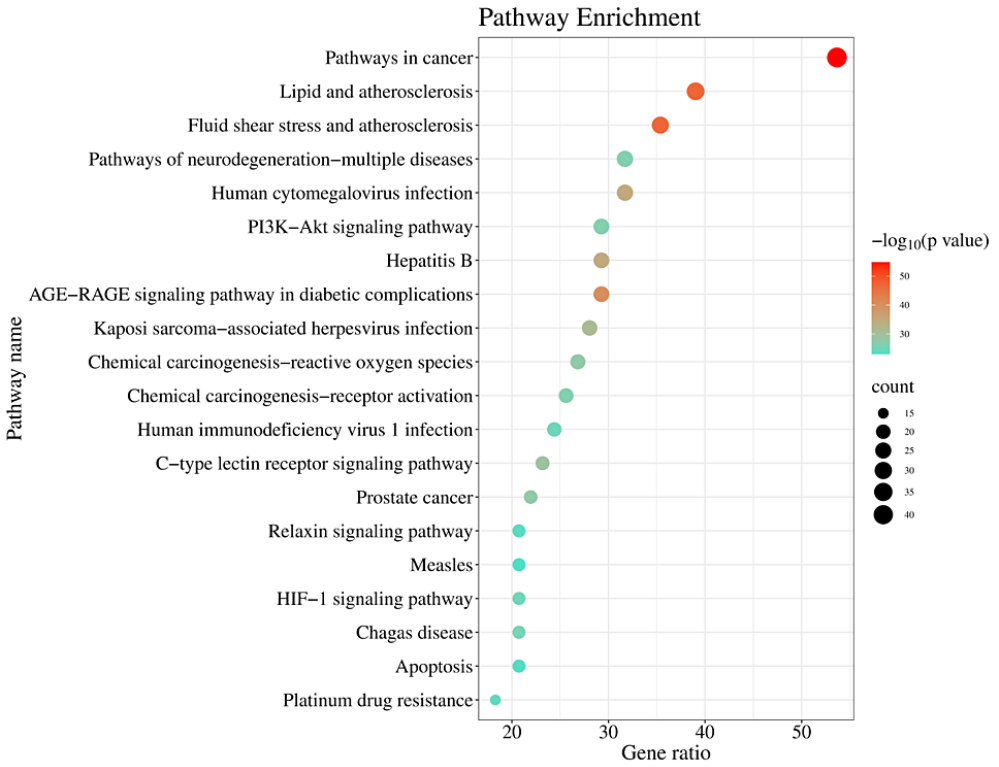

Fig. 4: The Kyoto Encyclopedia of Genes and Genomes pathway for the leaves of *Bergenia scopulosa* on oxidative damage

GO and KEGG Pathway Enrichment

The 82 candidate antioxidant genes identified from *B. scopulosa* were subjected to pathway and functional enrichment analysis using the Metascape database, with "human sapiens" set as the reference species. The top 10 significantly enriched biological processes, cellular components, and molecular functions (sorted by FDR values) were selected for visualization and detailed interpretation (Figure 3). Enrichment analysis revealed that the leaf-derived antioxidant targets of *B. scopulosa* are primarily associated with critical biological processes including: Positive regulation of protein phosphorylation and cell migration; response to oxidative stress and lipopolysaccharide stimulation. At the cellular component level, these proteins predominantly localize to perinuclear cytoplasmic regions, membrane rafts/microdomains, vesicular compartments (lumens of secretory granules, cytoplasmic vesicles) and caveolar structures. Molecular function analysis highlighted their involvement in enzymatic activities (oxidoreductase, nitric-oxide synthase regulator), protein-protein interaction domains (kinase binding, protein homodimerization), ligand-binding functions (heme, tetrapyrrole) and regulatory functions (enzyme activation, protein domain-specific binding). These findings collectively demonstrate that *B. scopulosa* leaf extracts modulate antioxidant responses through multiple regulatory pathways.

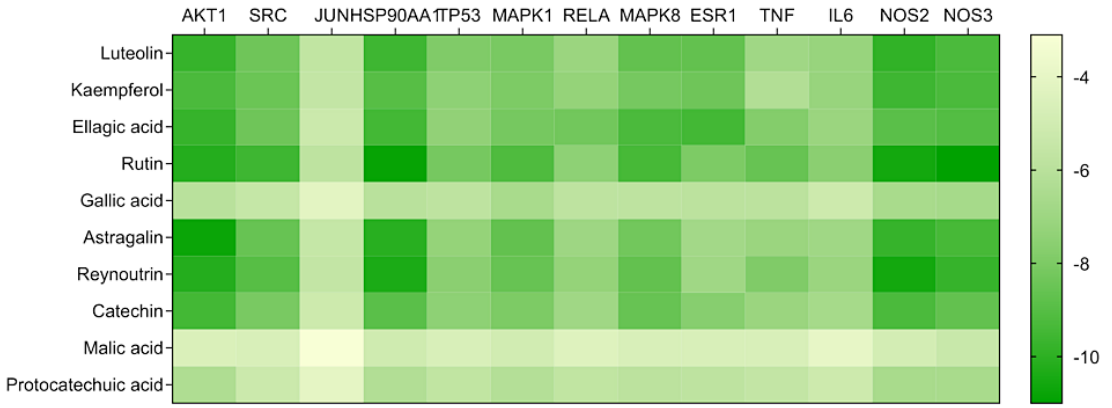

Fig. 5: Heat map of molecular docking binding energy

KEGG pathway enrichment analysis was conducted using the Metascape database to identify significantly associated pathways. The top 20 pathways with the lowest FDR were selected for visualization and interpretation (Figure 4). The graphical representation employs standardized parameters: Bubble size corresponds to the number of *B. scopulosa* leaf-derived antioxidant targets involved in each pathway; X-axis indicates the ratio of the targets involved in the pathway to the total number targets of the leaves of *B. scopulosa* on oxidative damage; color gradient from blue (low significance) to red (high significance) reflects pathway enrichment confidence. Pathway analysis revealed that *B. scopulosa* leaf extracts modulate antioxidant responses through multiple interconnected biological networks. Notably, the most significantly enriched pathways include cancer pathways, lipid and atherosclerosis, fluid shear stress and atherosclerosis, neurodegeneration-multiple diseases, human cytomegalovirus infection, PI3K-Akt signaling pathway, hepatitis B, AGE-RAGE signaling pathway in diabetic complications, Kaposi sarcoma-associated herpesvirus infection, chemical carcinogenesis-reactive oxygen species, etc. These findings establish a multi-dimensional regulatory network where *B. scopulosa* leaf antioxidants converge on critical pathophysiological processes.

Molecular Docking

According to the results of leave-compound-target and PPI network for the leaves of *B. scopulosa* on oxidative damage, molecular docking was performed among 10 bioactive compounds (luteolin, kaempferol, ellagic acid, rutin, gallic acid, astragalin, reynoutrin, catechin, malic acid, and protocatechuic acid) and 13 key targets (AKT1, SRC, JUN, HSP90AA1, TP53, MAPK1, RELA, MAPK8, ESR1, TNF, IL6, NOS2, and NOS3) using AutoDockTools 1.5.7 software. The PDB IDs of the key targets were listed in Table S4. The results of molecular docking analysis were listed in Table S6. Figure 5 reveals that luteolin, kaempferol, ellagic acid, rutin, astragalin, reynoutrin, and catechin exhibited significant docking interactions with 13 key antioxidant targets. Notably, luteolin, ellagic acid, rutin, astragalin, and reynoutrin demonstrated strong binding affinity towards AKT1 and HSP90AA1, while luteolin, kaempferol, rutin, astragalin, and reynoutrin showed preferential interactions with NOS2/NOS3. Ellagic acid exhibited the highest binding potency with ESR1 among all tested compounds. As shown in Figure 6A, luteolin formed five hydrophobic interactions with three residues (TRP, LEU, VAL), four hydrogen bonds with three residues (SER, THR, VAL) in AKT1. As shown in Figure 6B, rutin established seven hydrophobic interactions with four residues (TRP, VAL, LEU, LYS), six hydrogen bonds with three residues (ASN, GLN, TRP), two π-stacking (parallel) with TRP, one π-cation interaction with LYS in AKT1. As shown in Figure 6C, astragalin engaged eight hydrophobic interactions with four residues (TRP, LEU, LYS, VAL), seven hydrogen bonds with three residues (ASN, THR, SER), one π-stacking (parallel) with TRP in AKT1. As shown in Figure 6D, reynoutrin displayed five hydrophobic interactions with three residues (TRP, LEU, LYS), five hydrogen bonds with four residues (ASN, TRP, THR, SER), one π-stacking (parallel) with TRP in AKT1. As shown in Figure 6E, rutin formed two hydrophobic interactions with LEU and PHE, 7

hydrogen bonds with five residues (ASN, GLY, PHE, TRP, THR), two π-stacking (parallel) with PHE, two π-Stacking (perpendicular) with TRP in HSP90AA1. As shown in Figure 6F, astragalin established three hydrophobic interactions with LEU and PHE, six hydrogen bonds with four residues (ASN, GLY, LEU, THR), two π-stacking (parallel) with PHE, two π-stacking (perpendicular) with TRP in HSP90AA1. As shown in Figure 6G, reynoutrin showed two hydrophobic interactions with LEU and PHE, seven hydrogen bonds with five residues (ASN, GLY, PHE, TRP, THR), two π-stacking (parallel) with PHE, two π-stacking (perpendicular) with TRP in HSP90AA1. As shown in Figure 6H, ellagic acid formed one hydrophobic interaction with ESR1, four hydrogen bonds with four residues (ALA, ARG, HIS, LEU) in ESR1. As shown in Figure 6I, luteolin formed eight hydrophobic interactions with five residues (TRP, ALA, LEU, PHE, TYR), three hydrogen bonds with three residues (THR, ARG, SER), two π-stacking (parallel) with TRP in NOS2. As shown in Figure 6J, rutin established nine hydrophobic interactions with six residues (TRP, ALA, LEU, VAL, PHE, TYR), three hydrogen bonds with three residues (THR, ARG, GLY), three π-stacking (parallel) with TRP in NOS2. As shown in Figure 6K, astragalin engaged seven hydrophobic interactions with six residues (TRP, ALA, ARG, LEU, PHE, TYR), two hydrogen bonds with ASN and GLU, three π-stacking (parallel) with TRP and PHE in NOS2. As shown in Figure 6L, reynoutrin displayed nine hydrophobic interactions with five residues (TRP, ALA, LEU, PHE, TYR), three hydrogen bonds with three residues (ARG, SER, GLU), two π-stacking (parallel) with TRP in NOS2. As shown in Figure 6M, rutin formed six hydrophobic interactions with four residues (TRP, ALA, LEU, PHE), eleven hydrogen bonds with seven residues (ARG, SER, GLN, TYR, TRP, GLU, ASN), two π-stacking (parallel) with TRP in NOS3. As shown in Figure 6N, astragalin established five hydrophobic interactions with three residues (TRP, LEU, PHE), four hydrogen bonds with three residues (SER, TRP, GLU), two π-stacking (parallel) with TRP in NOS3. As shown in Figure 6O, reynoutrin showed six hydrophobic interactions with four residues (TRP, ALA, LEU, PHE), three hydrogen bonds with three residues (ARG, TRP, GLU), two π-stacking (parallel) with TRP in NOS3.

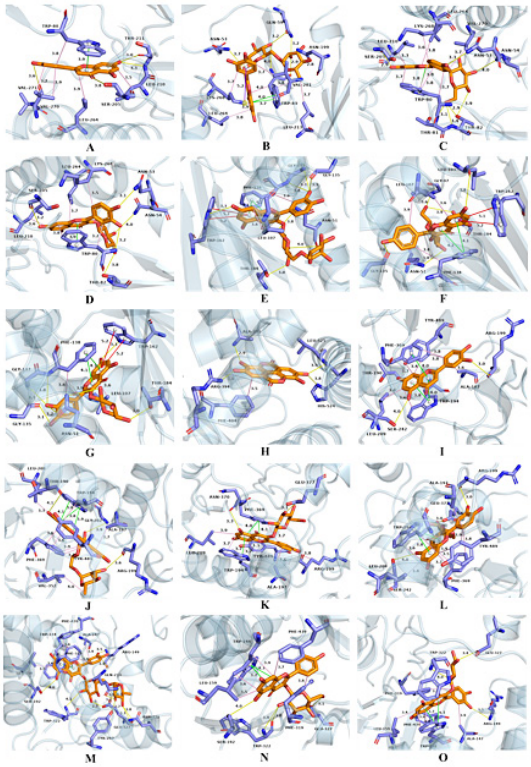

Fig. 6. Visualization of molecular docking. A. luteolin-AKT1; B. rutin-AKT1; C. astragalin-AKT1; D. reynoutrin-AKT1; E. rutin-HSP90AA1; F. astragalin-HSP90AA1; G. reynoutrin-HSP90AA1; H. ellagic acid-ESR1; I. luteolin-NOS2; J. rutin-NOS2; K. astragalin-NOS2; L. reynoutrin-NOS2; M. rutin-NOS3; N. astragalin-NOS3; O. reynoutrin-NOS3. pink: Hydrophobic Interaction; yellow: Hydrogen Bond; green: π-Stacking (parallel); red: π-Stacking (perpendicular); purple: π-Cation Interaction.

Discussion

Due to the influence of traditional Chinese medicine usage habits, most medicinal herbs are still limited to a single part of the plant, such as roots, rhizomes, leaves, flowers, fruits, seeds, etc., resulting in low utilization of the entire plant and significant waste of resources. Studying the medicinal value of non-medicinal parts of traditional Chinese medicine is of great significance for the comprehensive development and utilization of Chinese medicine resources. In recent years, there has been a

growing interest in exploring the different parts or non-medicinal components of TCM herbs.[25-27] For example, a previous study[25] demonstrated that the roots (medicinal part) and stems (non-medicinal part) of *Ampelopsis delavayana* share identical chemical profiles and bioactivities. This finding provides a theoretical rationale and scientific evidence for utilizing stems as a therapeutic component, which could potentially alleviate the current shortage of its medicinal resources. Similarly, Li *et al*.[26] reported that the essential oils extracted from both the aerial parts and roots of *Saposhnikovia divaricata* significantly inhibited the secretion of nitric oxide, interleukin-1β, interleukin-6, and tumor necrosis factor-α. These oils also effectively scavenged DPPH, ABTS, and hydroxyl free radicals and exhibited significant antiproliferative activity against HeLa and HCT-8 cell lines.

The genus *Bergenia* comprises 32 species of flowering plants, seven of which are found in China, offering significant ornamental, medicinal, and edible values.[2] *Bergenia* species are traditionally utilized in Ayurvedic preparations to address conditions such as bladder and kidney stones, piles, abnormal leucorrhea, and pulmonary infections.[2,28,29] Additionally, the leaves of B. crassifolia are commonly used in Russia and the Altai region to prepare health drinks or tea, while the young leaves are also consumed by the Buryats and Mongols as a tea.[2] In Chinese medicine, the rhizomes of *B. scopulosa*, primarily distributed in the Qinling Mountains, are employed to treat a range of ailments including acute and chronic enterogastritis, cough, hematemesis, hematochezia, edema, metrorrhagia, metrostaxis, leukorrhea, and more.[1,5] However, the leaves of *B. scopulosa* remain underutilized, leading to a substantial waste of resources. The excessive production of free radicals, including hydroxyl radicals, superoxide anions, singlet oxygen, and reactive oxygen species (ROS), can disrupt the balance between prooxidant and antioxidant systems in the body, contributing to various diseases such as rheumatism, inflammation, diabetes, and cancer.[30] To date, only Bao *et al*.[31] have characterized 94 lipophilic compounds in the aerial part of *B. scopulosa* using gas chromatography coupled with mass spectrometry (GC-MS), encompassing long-chain diolefins, long-chain fatty acids, and aldehyde ketones. Therefore, it is imperative to investigate the material basis of *B. scopulosa* leaves to explore their mechanisms against oxidative damage.

The UHPLC-Q Exactive Focus MS system, renowned for its high resolution (70,000 at m/z 200) and rapid data acquisition capabilities, has been widely adopted for the analysis of complex plant metabolites. Recently, we have applied this practical method for analyzing complex chemical compositions in plants.[21,32] In our study, this technology was employed to identify 59 compounds in *B. scopulosa* leaves, including 13 flavonoids, 7 isocoumarins, 35 phenolic acids, and 4 others. According to previous research, only the negative ion mode was used for analysis, as flavonoids, isocoumarins, and phenols exhibited better responses in this mode. This may be because these compounds tend to lose hydrogen and generate quasi-molecular ions ([M-H]-) or other characteristic ions in the negative ion mode.The leaves of *B. scopulosa* contain abundant and structurally diverse phenolic compounds and exhibit $DPPH^{\cdot}$ and $ABTS^{\cdot+}$ scavenging abilities comparable to those of trolox. Furthermore, network pharmacology is instrumental in predicting the bioactive components and targets of *B. scopulosa* leaves in relation to oxidative damage. In this study, ten constituents in the leaves of *B. scopulosa* were screened as potential bioactive ingredients in the L-C-T network, and the PPI network identified 13 hub targets. The identification of 13 high-centrality proteins, including Nrf2 activators and MAPK kinases, reveals a systems-level antioxidant strategy in *B. scopulosa* through the coordinated regulation of ROS scavenging enzymes, redox sensors , and transcription factors to orchestrate enzymatic detoxification and gene expression responses. The L-C-T network identifies ten bioactive compounds (e.g., gallic acid, luteolin) targeting multiple pathways (NF-κB, Nrf2) to mitigate oxidative damage in chronic diseases, bridging phytochemical insights with translational potential. KEGG pathway analysis revealed that the leaves of *B. scopulosa* alleviate oxidative damage by regulating multiple pathways, such as those involved in cancer, lipid and atherosclerosis, fluid shear stress and atherosclerosis, neurodegeneration-multiple diseases, human cytomegalovirus infection, PI3K-Akt signaling pathway, hepatitis B, AGE-RAGE signaling pathway in diabetic complications, Kaposi sarcoma-associated herpesvirus infection, and chemical

carcinogenesis-reactive oxygen species, among others. These pathways collectively underlie the plant's protective effects against chronic diseases, including atherosclerosis, neurodegeneration, and diabetic complications. Notably, the activation of PI3K-AKT and NF-κB pathways suggests dual regulatory roles in both antioxidant defense and immune modulation. Additionally, molecular docking results demonstrated that luteolin, ellagic acid, rutin, astragalin, and reynoutrin exhibited strong binding activities with AKT1 and HSP90AA1. Luteolin, kaempferol, rutin, astragalin, and reynoutrin also showed strong binding affinities for NOS2 and NOS3. Among them, ellagic acid demonstrated exceptional binding specificity for ESR1. Compared with previous studies, our research coupled UHPLC-Q Exactive Focus MS, network pharmacology and molecular docking methods, demonstrated the potent antioxidant capacity of the rich phenolic components in *B. scopulosa*. These findings not only enrich the understanding of the medicinal value of *B. scopulosa*, but also provide a scientific basis for the development of new natural drugs.

Current studies reveal that flavonoids and phenolic acids exhibit diverse antioxidant and anti-inflammatory properties across multiple experimental models. Luteolin alleviated streptozotocin-induced diabetic cardiopathy in mice through Nrf2-mediated oxidative stress reduction and NF-κB-regulated inflammatory suppression.[33] Ellagic acid mitigated UVA-induced oxidative stress and apoptosis in human keratinocyte (HaCaT) cells via HO-1/Nrf-2/SOD upregulation,[34,35] while also improving cognitive function and reducing inflammatory markers in aged rats.[36] Rutin enhanced SOD/CAT/GPx activity and reduced 6-OHDA-induced lipid peroxidation in PC12 cells.[37] Astragalin reduced malondialdehyde accumulation and elevates superoxide dismutase/catalase activities in carrageenan-injected mice, demonstrating broad-spectrum antioxidant efficacy.[38] Kaempferol activated the Nrf2/SLC7A11/GPX4 signaling pathway, enhanced antioxidant capacity, and reduced lipid peroxidation in neurons subjected to oxygen-glucose deprivation/reperfusion.[39] Reynoutrin suppressed TNF-α/IL-6/MDA levels, restored SOD activity, and attenuated myocardial fibrosis in ischemic heart failure rats.[40] The compounds identified in our study may play a role in the prevention or management of oxidative stress-related diseases through multiple mechanisms. For instance, some compounds may activate the antioxidant defense system by modulating the Nrf2 signaling pathway, thereby reducing oxidative stress. In addition, these compounds may also exert positive effects on diseases such as atherosclerosis, neurodegenerative diseases, and diabetes by inhibiting inflammatory responses and regulating apoptosis or autophagy.

The current study suggests that *B. scopulosa* leaf extracts may hold promise for treating oxidative stress-related diseases. However, several limitations should be noted: first, the lack of in vivo validation limits the understanding of their actual biological effects in whole organisms; second, the current compound identification accuracy relies primarily on chromatographic techniques, which may not fully resolve low-abundance or structurally similar metabolites. Future research should focus on conducting in vivo experiments to verify the pharmacological effects of these compounds and further assess their efficacy and safety through animal models and clinical trials. Additionally, more in-depth mechanistic studies are recommended to explore how these compounds exert their biological effects by modulating cellular signaling pathways and metabolic networks. Moreover, conducting quality control studies on *B. scopulosa* is essential to ensure consistency in herbal medicine applications. Future research could also focus on the extraction and optimization of these compounds, and as well as testing their efficacy in pharmaceutical or nutraceutical contexts.

Conclusion

The current study employed UHPLC-Q Exactive Focus MS to comprehensively identify 59 compounds in *B. scopulosa* leaves, including 13 flavonoids, [7] isocoumarins, 35 phenolic acids, and 4 additional compounds. Notably, all these known compounds were reported from the leaves of *B. scopulosa* for the first time. The leaves exhibited a rich phenolic profile with structural diversity, demonstrating comparable antioxidant capacities to trolox through DPPH• and $ABTS^{\cdot+}$ scavenging assays. Network pharmacology and molecular docking analyses revealed that the primary bioactive compounds responsible for oxidative damage attenuation in *B. scopulosa* leaves are astragalin, reynoutrin, rutin, luteolin, ellagic acid, kaempferol, and catechin. These findings suggest that *B. scopulosa* leaf

extracts may offer therapeutic potential for oxidative stress-related diseases, including atherosclerosis, neurodegeneration, inflammation, and diabetic complications. This research not only advances our understanding of the phytochemical basis of *B. scopulosa*'s medicinal value but also provides new perspectives for the development of standardized herbal therapies derived from underutilized plant parts. The integrated approach of metabolomics, bioinformatics, and molecular modeling highlights a promising strategy for exploring multifaceted drug candidates in traditional medicinal plants. Further investigations, such as mechanistic studies, toxicity evaluations, and pharmacokinetic profiling, are essential for a comprehensive understanding and optimized utilization of *B. scopulosa* leaves as a medicinal resource.

Acknowledgement
The authors are profoundly grateful to the Science and Technology Department of Shaanxi Province and Shaanxi Administration of Traditional Chinese Medicine for their financial support of this research.

Funding Sources
This work was supported by the Key Research and Development Program of Shaanxi (No. 2022SF-544), the Project of Shaanxi Administration of Traditional Chinese Medicine (No. 2022-SLRH-YQ-003, SZY-KJCYC-2025-JC-051).

Conflict of Interest
The authors do not have any conflict of interest.

Data Availability Statement
Data will be made available on request.

Ethics Statement
This study did not involve human participants, animal subjects, and any material that requires ethical approval.

Informed Consent Statement
This study did not involve human participants, and therefore, informed consent was not required.

Clinical Trial Registration
This research does not involve any clinical trials.

Permission to Reproduce Material from Other Sources
Not Applicable.

Author Contributions
- **Hui Ren:** Conceptualization, Methodology, Analysis, Writing- Original Draft.
- **Wenjing Lu:** Methodology, Analysis, Writing-Original Draft & Review
- **Hui Ren and Wenjing Lu:** Have contributed equally to this work and share first authorship.
- **Xiaomin Cui:** Methodology, Writing – Editing.
- **Jing Hu:** Data Collection, Analysis, Writing – Editing.
- **Zhiyong Chen:** Conceptualization, Supervision.

References

1. Guo L., Xu Y., Li Y., Zhang D., Huang W., Deng C., *et al*. Quality evaluation of the rhizomes of *Bergenia scopulosa*. *J Shaanxi Univ Chin Med.* 2021; 44(6): 61-66.
2. Koul B., Kumar A., Yadav D., Jin J.O. *Bergenia* genus: Traditional uses, phytochemistry and pharmacology. *Molecules.* 2020; 25(23): 5555.
3. Ren H., Hu J., Cui X., Lu W., Li N., Qu T., *et al*. Quality evaluation of *Bergenia*e Scopulosae Rhizoma based on fingerprints combination with chemical pattern recognition and content determination of phenolic compounds. *Chin Tradit Herb Drugs.* 2023; 54(19): 6452-6460.
4 Mao S., Li Q., Li Y., Wang Y., Zhou Y. Research advances on the rare and endangered plant *Bergenia scopulosa*. *Guangxi Forest Sci.* 2017; 46(4): 396-399.
5. Ren H., Lu W., Cui X., Hu J., Li N., Qu T., *et al*. Analysis of prototype components and metabolites from *Bergenia*e Scopulosae Rhizoma absorbed into blood by UHPLC-Q Exactive Focus MS/MS. *Chin J Exp Tradit Med Form*. 2023; 29 (1): 113-122.
6. Cui Y. Chemical constituents from *Bergenia scopulosa* (I). *Chin Tradit Pat Med*. 2011;

33(9): 1546-1549.
7. Cui Y. Chemical constituents from rhizomes of *Bergenia scopulosa* (II). *Chin Tradit Herb Drugs.* 2012; 43(9): 1704-1707.
8. Lv X., Wang J. Study on the chemical constituents from *Bergenia scopulosa* (I). *J Chin Med Mater*. 2003; (11): 791-792.
9. Ren H., Cui X., Hu J., Liu X., Chen Z. Analysis on chemical constituents in rhizomes of *Bergenia scopulosa* by UHPLC-Q Exactive Focus MS/MS. *Chin J Exp Tradit Med Form.* 2021; 27(9): 118-128.
10. Wang J., Lv X. Study on the chemical constituents from *Bergenia scopulosa* (I). *J Chin Med Mater.* 2005; 28(1): 23-24.
11. Wei Y. Chemical Constituents from *Bergenia scopulosa* (I). *Chin J Exp Tradit Med Form.* 2012; 18(9): 154-156.
12. Gao W., Yin Q., Wang X., Teng X., Jin R., Liu N., *et al*. UHPLC-Q-Exactive Orbitrap mass spectrometry reveals the lipidomics of bovine milk and yogurt. *Food Chem.* 2022; 392: 133267.
13. Jin Y., Cheng S., Liu R., Yu C., Zhang L., Li X.L., *et al*. Comprehensive characterization of the chemical composition of Lurong dabu decoction and its absorbed prototypes and metabolites in rat plasma using UHPLC-Q Exactive Orbitrap-HRMS. *Food Res Int.* 2022; 161: 111852.
14. Xue Q., Fan H., Li K., Yang L., Sun L., Liu Y. Comparative evaluations on phenolic antioxidants of nine adulterants and anti-inflammation of four alternatives with their original herb Erycibe schmidtiit. *RSC advances*, 2017; 7: 51151
15. He J., Shang F., Li L., Song X., Yang Y., Zhang X., *et al*. Establishment of fingerprints and spectrum-effect relationship of antioxidant activity of *Citri Sarcodactylis Fructus. Chin Tradit Herb Drugs.* 2023; 54(23): 7841-7852.
16. Ru J., Li P., Wang J., Zhou W., Li B., Huang C., *et al*. TCMSP: a database of systems pharmacology for drug discovery from herbal medicines. *J Cheminformatics.* 2014; 6: 13.
17. Daina A., Michielin O., Zoete V. SwissTargetPrediction: updated data and new features for efficient prediction of protein targets of small molecules. *Nucleic Acids Res.* 2019; 47(W1): W357-W364.
18. Gfeller D., Grosdidier A., Wirth M., Daina A., Michielin O., Zoete V. Swiss Target Prediction: a web server for target prediction of bioactive small molecules. *Nucleic Acids Res.* 2014; 42: W32-W38.
19. Stelzer G., Rosen N., Plaschkes I., Zimmerman S., Twik M., Fishilevich S., *et al*. The GeneCards suite: from gene data mining to disease genome sequence analyses. *Curr Protoc Bioinform.* 2016; 54: 1.30.1-1.30.33.
20. Szklarczyk D., Franceschini A., Wyder S., Forslund K., Heller D., Huerta-Cepas J., *et al*. STRING v10: protein-protein interaction networks, integrated over the tree of life. *Nucleic Acids Res.* 2015; 43: D447-D452.
21. Cui X., Hu J., Chen Z., Ren H. Qualitative analysis and quality evaluation of Pimpinella thellungiana by serum pharmacochemistry, network pharmacology, and QAMS. *J AOAC Int.* 2022; 106(1): 179-191.
22. Ye C., Li N., Chen Y., Qu T., Hu J., Chen Z., *et al*. Exploring mechanism of Porana racemosa Roxb. in treating rheumatoid arthritis based on integration of network pharmacology and molecular docking combined with experimental validation. *Acta Pharm Sin.* 2025; 60(1): 117-129.
23. Salentin S., Schreiber S., Haupt V.J., Adasme M.F., Schroeder M. PLIP: fully automated protein-ligand interaction profiler. *Nucleic Acids Res.* 2015; 43(W1): W443-W447.
24. Pisoschi A.M., Pop A. The role of antioxidants in the chemistry of oxidative stress: A review. *Eur J Med Chem.* 2015; 97: 55-74.
25. Li B., Yang Z., Mao F., Wang Q., Fang H., Gu X., *et al*. Phytochemical profile and biological activities of the essential oils in the aerial part and root of Saposhnikovia divaricata. *Sci Rep.* 2023; 13(1): 8672.
26. Qiong J., Yang H., Xie Y., Zhu P., Chen G., Zhou Q., *et al*. Evaluation of comparative chemical profiling and bioactivities of medicinal and non-medicinal parts of Ampelopsis delavayana. *Heliyon.* 2024; 10(12): e32408.
27. Zhao Q., Li Y., Li S., He X., Gu R. Comparative bioactivity evaluation and metabolic profiling of different parts of Duhaldea nervosa based on GC-MS and LC-MS. *Front Nutr.* 2023; 10: 1301715.
28. Ahmad M., Butt M.A., Zhang G., Sultana S., Tariq A., Zafar M. *Bergenia* ciliata: A comprehensive review of its traditional uses,

phytochemistry, pharmacology and safety. *Biomed pharmacother.* 2018; 97: 708-721.
29. Srivastava S., Rawat A.K.S. Botanical and phytochemical comparison of three *Bergenia* species. *J Sci Ind Res.* 2008; 67: 65-72.
30. Riaz A., Rasul A., Hussain G., Zahoor M.K., Jabeen F., Subhani Z., *et al*. Astragalin: A bioactive phytochemical with potential therapeutic activities. *Adv Pharmacol Sci.* 2018; 2018: 9794625.
31. Bao H., Zhu Y., Aikebaier K., Qinyihe K., Wang J. Studies on the chemical constituents from the aerial part of *Bergenia scopulosa* T. P. Wang. *Northwest Pharm J.* 2013; 28(2): 125-129.
32. Li N., Du X., Qu T., Ren H., Lu W., Cui X., *et al*. Pharmacodynamic material basis and pharmacological mechanisms of Cortex Mori against diabetes mellitus. *J Ethnopharmacol.* 2024; 324: 117781.
33. Li L., Luo W., Qian Y., Zhu W., Qian J., Li J., *et al*. Luteolin protects against diabetic cardiomyopathy by inhibiting NF-κB-mediated inflammation and activating the Nrf2-mediated antioxidant responses. *Phytomedicine.* 2019; 59: 152774.
34. Hseu Y.C., Chou C.W., Senthil Kumar K.J., Fu K.T., Wang H.M., Hsu L.S., *et al*. Ellagic acid protects human keratinocyte (HaCaT) cells against UVA-induced oxidative stress and apoptosis through the upregulation of the HO-1 and Nrf-2 antioxidant genes. *Food Chem Toxicol.* 2012; 50(5): 1245-1255.
35. Zhu H., Yan Y., Jiang Y., Meng X. Ellagic acid and its anti-aging effects on central nervous system. *Int J Mol Sci.* 2022; 23(18): 10937.
36. Chen P., Chen F., Zhou B. Antioxidative, anti-inflammatory and anti-apoptotic effects of ellagic acid in liver and brain of rats treated by D-galactose. *Sci Rep.* 2018; 8(1): 1465.
37. Enogieru A.B., Haylett W., Hiss D.C., Bardien S., Ekpo O.E. Rutin as a potent antioxidant: Implications for neurodegenerative disorders. *Oxid Med Cell Longev.* 2018; 2018: 6241017.
38. Alblihed M.A. Astragalin attenuates oxidative stress and acute inflammatory responses in carrageenan-induced paw edema in mice. *Mol Biol Rep.* 2020; 47(9): 6611-6620.
39. Yuan Y., Zhai Y., Chen J., Xu X., Wang H. Kaempferol ameliorates oxygen-glucose deprivation/reoxygenation-induced neuronal ferroptosis by activating Nrf2/SLC7A11/GPX4 axis. *Biomolecules.* 2021; 11(7): 923.
40. Yang W., Tu H., Tang K., Huang H., Ou S., Wu J. Reynoutrin improves ischemic heart failure in rats via targeting S100A1. *Front Pharmacol.* 2021; 12: 703962.